IEEE Photonics Journal
An IEEE Photonics Society Publication

Open Access

Nonlinearity Mitigation Based on Modulus Pruned Look-Up Table for Multi-Bit Delta-Sigma 32-CAP Modulation in Underwater Visible Light Communication System

Volume 13, Number 1, February 2021

Wenqing Niu
Hui Chen
Junwen Zhang
Yinaer Ha
Peng Zou
Nan Chi

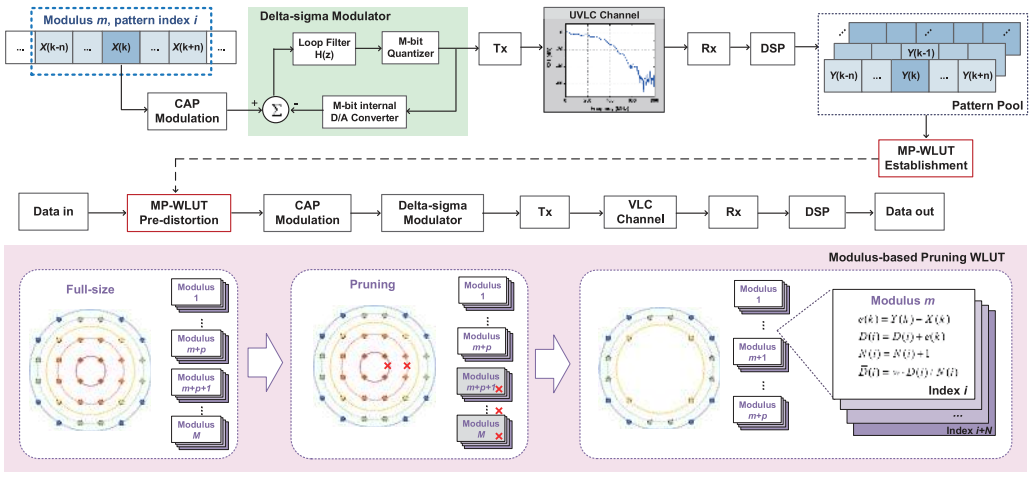

DOI: 10.1109/JPHOT.2021.3050753

Nonlinearity Mitigation Based on Modulus Pruned Look-Up Table for Multi-Bit Delta-Sigma 32-CAP Modulation in Underwater Visible Light Communication System

Wenqing Niu, Hui Chen, Junwen Zhang, Yinaer Ha, Peng Zou, and Nan Chi

Key Laboratory for Information Science of Electromagnetic Waves (MoE), Fudan University, Shanghai 200433, China

DOI:10.1109/JPHOT.2021.3050753

Manuscript received December 17, 2020; accepted January 5, 2021. Date of publication January 14, 2021; date of current version February 1, 2021. This work was supported in part by the National Key Research and Development Program of China under Grant 2017YFB0403603 and in part by the NSFC project under Grants 61925104 and 62031011. Corresponding author: Nan Chi (e-mail: nanchi@fudan.edu.cn).

Abstract: Application of light-emitting diodes (LEDs) based visible light communication (VLC) in underwater wireless communication has become a hot topic. However, on the one hand, the performance of underwater VLC (UVLC) system is limited due to power attenuation in water medium. On the other hand, increasing the driving power will induce nonlinearity from the imperfect optoelectronic components. Particularly at high signal amplitude, nonlinearity will become the dominant bottleneck. In this paper, we focus on nonlinearity mitigation method which preprocesses signal at transmitter-side. Multi-bit delta-sigma modulation combined carrier-less amplitude and phase modulation (DSM-CAP) is proposed to obtain quantized signal with lower peak-to-average power ratio (PAPR). Furthermore, as assuming the quantization noise being additive white noise is not appropriate in nonlinearity, modulus pruned weighted look-up table (MP-WLUT) is employed to modify the signal before DSM quantization to mitigate pattern dependent nonlinear distortion. Experimental results indicate that the DSM-CAP has better nonlinearity mitigating performance than normal CAP. At the data rate of about 1.69Gbp/s, utilizing MP-WLUT pre-distorted DSM-CAP an improvement of 1.44 dB Q-factor is realized compared with normal CAP without WLUT, and the size of MP-WLUT can be reduced to 62.5% of the full-size WLUT.

Index Terms: Underwater visible light communication, delta-sigma modulation, look-up table, nonlinearity mitigation.

1. Introduction

In recent years, with the rapid development of ocean exploration, the demand for high-speed underwater data transmission is increasing. Existing underwater wireless communication methods such as acoustic communication and radio frequency (RF) communication have their own limitations due to low bandwidth and high attenuation, respectively. It is reported that visible light has a low attenuation window at the blue-green spectra region in water, providing gigabit-per-second order of magnitude transmission speed [1]. Therefore, underwater visible light communication has been

considered as a potential alternative and attracted scholars' attention all over the world [2]–[6]. Owing to the incoherent characteristics of LED, only intensity modulation and direct detection scheme is employed in LED-based UVLC system, so that the value of transmitted signal is restricted to be real. Carrier-less amplitude and phase (CAP) modulation is a widely investigated modulation format which utilizes a pair of orthogonal shaping filters to realize complex-to-real-value conversion [7]–[12]. Since signal in water medium will suffer significant attenuation due to absorption, scattering and turbulence, higher driving bias is required to improve the signal-to-noise ratio (SNR), which will in turn induces nonlinear distortion due to the imperfect optoelectronic components such as LED, photodetector, electrical amplifier and other components of the circuits [13]. Additionally, the impact of nonlinearity becomes severe for signal with high amplitude. Under average power constraints, signal with higher PAPR is more susceptible to nonlinear distortion, which is a non-trivial problem in UVLC system.

Delta-sigma modulation (DSM) is known as a high-precision data converter for quantizing continuous waveform into discrete levels. DSM can offer robustness against noise and lower PAPR through oversampling and noise shaping [14], [15], which has been investigated experimentally in orthogonal-frequency division multiplexing (OFDM) visible light communication (VLC) system. However, existing DSM applications in VLC only involve low quantization levels (1-bit or 2-bit) [16], [17]. In order to mitigate quantization noise, quite high oversampling rate is needed which would lead to strict demand for transmitting device in high speed UVLC system. It is also noted that the output of DSM quantizer is based on the theory that quantization noise is additive white noise [18], yet disregarding the prior knowledge of channel characteristics. Look-up table (LUT) is a nonlinear digital pre-distortion algorithm which records the average pattern dependent distortion of the channel and could compensate the impairment by nonlinear predistortion [19]. Inspired by [18], we consider employing LUT to modify the signal according to pattern of successive symbols before DSM quantization. However, the complexity of LUT grows rapidly as CAP order increases. The implementation of high-order CAP remains challenging. Researches indicate that the nonlinear distortion of CAP modulation in LED-based UVLC system is related to modulus values of constellations, which means symbols at outer modulus are more nonlinearly distorted [9]–[11].

Considering the feature of CAP constellation, in this paper, we propose to combine the multi-bit DSM-CAP with modulus pruned weighted look-up table (MP-WLUT) to preprocess the transmitting signal, and the concept of pruning the LUT by abandoning symbols of inner modulus with less distortion is presented for the first time, so that the size of LUT could be reduced and meanwhile maintain sub-optimal performance. In addition, the pre-distortion vector in LUT is weighted. Therefore, the proposed MP-WLUT pre-distorted multi-bit DSM-CAP high-speed UVLC system is demonstrated. Experimental results show that DSM-32-CAP outperforms normal 32-CAP when facing strong nonlinearity. At the bandwidth of 337.5 MHz and data rate of about 1.69 Gbps, the Q factor of MP-WLUT pre-distorted 4-bit DSM-CAP is increased by 1.44 dB compared with normal CAP without WLUT, just 0.15 dB less than that of full-size WLUT pre-distorted DSM-CAP, while the size of MP-WLUT is significantly decreased to 62.5% of full-size WLUT.

2. Principle

In this section, we will first give a brief introduction of underwater VLC channel, and then the schematic of the proposed MP-WLUT pre-distorted DSM-CAP system will be illustrated. Afterwards, principle of the two key components: delta-sigma modulation and modulus pruned WLUT will be introduced in detail.

2.1 Underwater Visible Light Communication Channel

The implementation of UVLC system remains a challenge because signal transmitted in the communication links will suffer from detrimental effects from underwater optical channel and optoelectronic components. In underwater optical channel, absorption, scattering, and turbulence

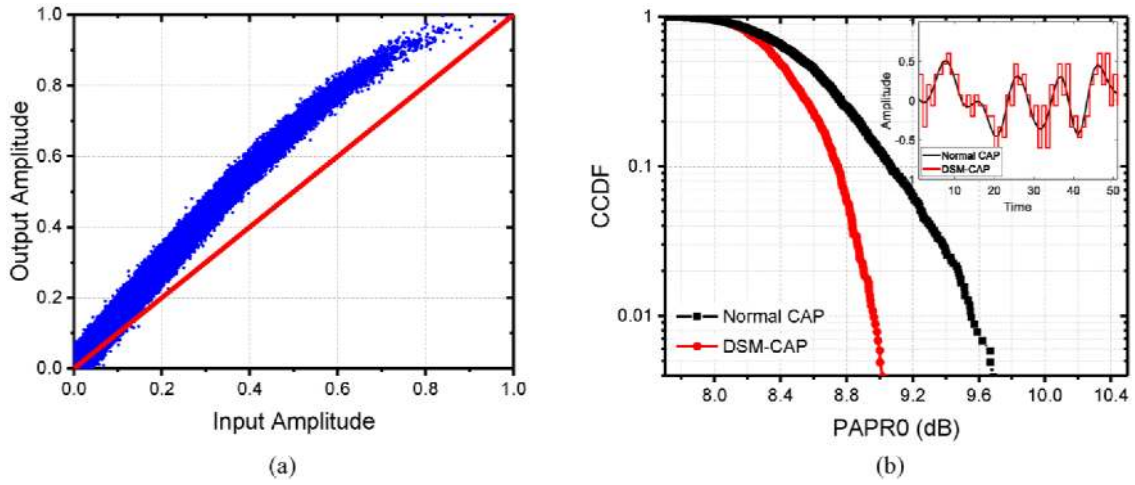

Fig. 1. (a) The nonlinear response of UVLC system. (b) CCDF of normal CAP and DSM-CAP. Inset: The waveform of normal CAP and DSM-CAP.

are the three main factors. Firstly, absorption is the inevitably power attenuation in water medium, and it will lead to decrease of signal-to-noise ratio (SNR). Secondly, scattering means the deflection of light from original path as it propagates in water, and it corresponds to interaction between photon and microcosmic particle such as molecule or atom at the micro-level. The scattering properties of the medium depend on structure, types, and concentrations of particles [20]. Thirdly, turbulence refers to changes in the refractive index of water which is related to fluctuations in temperature, salinity, and pressure. It will introduce instantaneous fluctuations over the average power [21].

Apart from optical channel, defect of optoelectronic components also introduce impairment to the signal. As the amplitude of signal increases, nonlinear effect will gradually dominate the performance of the system as a result of the nonlinear electro-optical conversion of LED and saturation effect of photodiode at the receiver-side. The nonlinear response of other electrical components such as electronic driver at the transmitter-side and trans-impedance amplifier (TIA) at the receiver-side is also the source of nonlinearity. The nonlinear response is illustrated in Fig. 1(a). The input amplitude and output amplitude are normalized. Apparently, when input amplitude exceeds certain value, the output amplitude is no more linear.

2.2 MP-WLUT Pre-Distorted DSM-CAP System

Nonlinear effect will introduce distortion especially at high input amplitude and the nonlinear model is difficult to fit. Therefore, nonlinearity has become one of the major limitations of system performance. Aimed at avoiding complexity increase at the receiver-side, pre-equalization or signal preprocessing is preferred. Under average power constraints, PAPR is a measure of resistance to nonlinearity. Signal with lower PAPR is more suitable for system where there is strong nonlinearity. Delta-sigma modulation is a well-known data converter. In this paper, DSM is employed to quantize CAP signal into discrete levels. As Fig. 1(b) shows, DSM-CAP obtains lower PAPR than normal CAP, and thus DSM-CAP is supposed to offer superior performance in UVLC system. The waveform of normal CAP and DSM-CAP in time domain is inserted. In general, the output of DSM is based on the theory that quantization noise is additive white noise and is optimal in additive white Gaussian noise (AWGN) channel. However, bandwidth limitation and nonlinearity exist in UVLC channel, resulting in inter-symbol interference (ISI) and nonlinear distortion. It's necessary to take the prior knowledge of channel into account. Therefore, we propose to use MP-WLUT pre-distorted multi-bit DSM-CAP in UVLC system. The schematic is shown in Fig. 2.

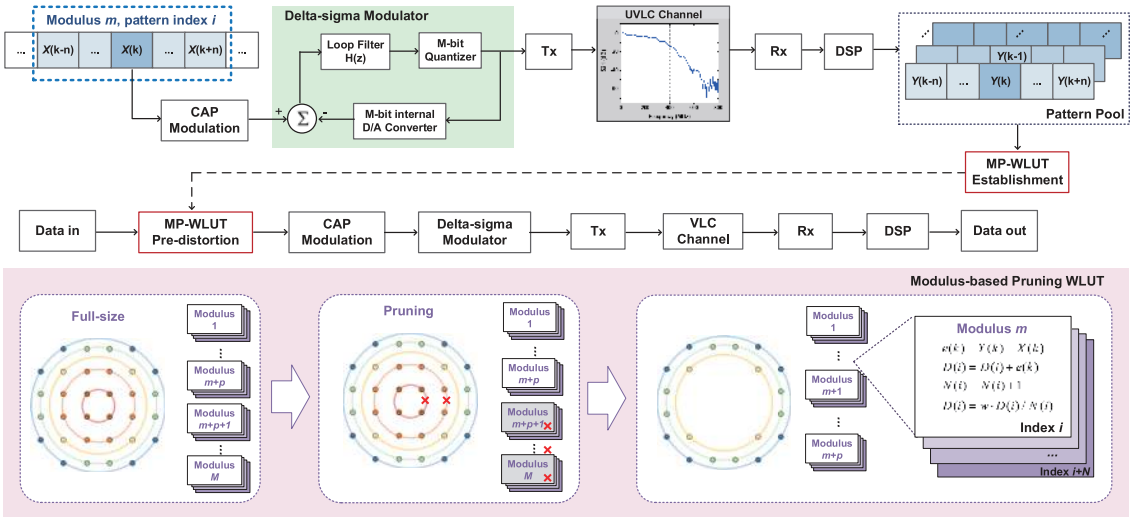

Fig. 2. Schematic of MP-WLUT pre-distorted DSM-CAP system.

Firstly, to establish MP-WLUT, the original quadrature amplitude modulation (QAM) data is modulated to CAP signal. Every continuous $2n+1$ symbols in a sliding window correspond to a pattern, and the index of the pattern is i. A delta-sigma modulator is employed to quantize the CAP signal. Then the DSM-CAP signal is transmitted. After UVLC channel, the received signal is sent into primary DSP block. Then the received sequence forms a pattern pool, and the pattern dependent distortion will be recorded in MP-WLUT. Afterwards, for new input data, the middle symbol in a sliding window is pre-distorted according to the pattern index. Then the signal is modulated and transmitted as the process stated above.

2.3 Delta-Sigma Modulation

In this paper, multi-bit DSM is employed to quantize the amplitude of CAP signal from continuous levels to fewer discrete levels. The main idea of DSM is oversampling and noise-shaping. On the one hand, oversampling could spread the quantization noise over a wide frequency range, so that the in-band noise could be reduced. On the other hand, noise-shaping scheme is employed to push the quantization noise out of the signal band. Through the above techniques, the in-band quantization noise could be significantly reduced.

The block diagram of DSM is shown in Fig. 2. It consists of a loop filter $H(z)$ and a quantizer $q(n)$ embedded in a feedback loop. According to [22], the signal transfer function (STF) and noise transfer function (NTF) could be expressed as:

$$STF(z) = \frac{H(z)z^{-1}}{1 + H(z)z^{-1}} \tag{1}$$

$$NFT(z) = \frac{1}{1 + H(z)z^{-1}} = 1 - STF(z) \tag{2}$$

When designing $H(z)$, the in-band signal components should not be spectrally altered. $H(z)$ is typically a cascade of integrators. For simplicity, suppose $H(z)$ with N poles and $N-1$ zeros:

$$H(z) = \frac{\sum_{i=0}^{N-1} a_i z^{-i}}{(1 - z^{-1})^N} \tag{3}$$

where a_i is constant, determining the gain and locations of the zeros of $H(z)$. Then the NTF can be rewritten as:

$$NTF(z) = \frac{(1-z^{-1})^N}{(1-z^{-1})^N + \sum_{i=0}^{N-1} b_i z^{-i-1}} \tag{4}$$

Apparently, the poles of $H(z)$ become zeros of NTF, and therefore, the NTF displays high-pass frequency response. Likewise, according to (2), STF displays low-pass frequency. As a result, through the loop filter, the in-band signal is remained and the quantization noise is pushed to high frequency. In [ref. [13], [15] and [16], [17], the applied DSM only involves a few quantization bits. In this case, to suppress quantization noise, higher oversampling rate is needed. Therefore, the desired sampling rate of DAC will grow rapidly, which requires DAC with high speed. However, due to the quantization operation, the requirement of resolution is tolerant in turn. It is necessary to make a compromise. Furthermore, the signal bandwidth will not be changed when the baud rate is fixed, and thus the requirement of ADC of receiver-side remains unchanged.

2.4 Modulus Pruned WLUT Pre-Distortion

WLUT is first proposed in [19]. As for any transmitted symbol sequence $X(k-n:k:k+n)$ in a sliding window (length 2n + 1) has a pattern index i , and the corresponding received signal $Y(k-n:k:k+n)$ shares the same index. The distortion of middle symbol in pattern i is denoted as $e(k)$:

$$e(k) = Y(k) - X(k) \tag{5}$$

The $e(k)$ is recorded in the look-up table with address i. As the sliding window moves forward, the middle symbol's distortion is recorded in corresponding address. Finally, the weighted average distortion $\tilde{D}(i)$ of pattern i is obtained:

$$\tilde{D}(i) = w \cdot \frac{D(i)}{N(i)} \tag{6}$$

where $D(i)$ is the summary of recorded distortion of pattern i, and $N(i)$ is the occurrence of pattern i. w is a constant which is used to adjust the weight of pre-distortion. Likewise, for any $X(k-n:k:k+n)$ corresponding to pattern i, the middle symbol in the pattern is pre-distorted by minus the weighted average distortion in WLUT. The pre-distorted transmitted signal is denoted as $\tilde{X}(k)$:

$$\tilde{X}(k) = X(k) - \tilde{D}(i) \tag{7}$$

As for q-CAP, various combinations will form a pattern pool containing q^{2n+1} patterns. The rapidly growth of WLUT complexity is a major barrier to implementation of WLUT for high-order CAP. Since abundant researches indicate that nonlinear distortion exists mostly in points at outer modulus of CAP constellations, we present a modulus pruned WLUT. The schematic is illustrated in Fig. 2. The pattern index in WLUT could be divided into M groups according to modulus of middle symbol in pattern. For 32-CAP, M equals to 5. Taking Modulus $m+p$ as boundary, the patterns of which the middle symbol belonging to inner modulus (modulus index from $m+p+1$ to M) are pruned. Finally, only patterns of outer modulus are remained and the size of WLUT is reduced. In pre-distortion phase, likewise, only symbols at outer modulus will be pre-distorted.

3. Experimental Setup

Fig. 3 shows the experimental setup of the proposed MP-WLUT pre-distorted DSM-CAP UVLC system. This system consists of two phases: the table establishing phase and signal predistortion phase. In the MP-WLUT establishing phase, the original data is mapped to 32-QAM signal, and then is up-sampled. The selection of up-sampling rate is related to parameters of DSM. After I/Q separation, in-phase and Quadrature Components pass through a pair of orthogonal shaping filter (Root raised cosine roll-off filter, the roll-off factor equals to 0.205) to produce CAP signal. And then implement delta-sigma modulation, so that the amplitude of CAP signal is converted into discrete

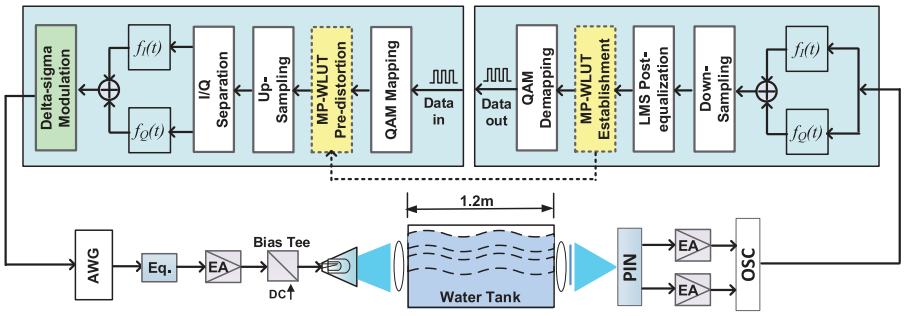

Fig. 3. Experimental setup of MP-WLUT pre-distorted DSM-CAP underwater visible light communication system.

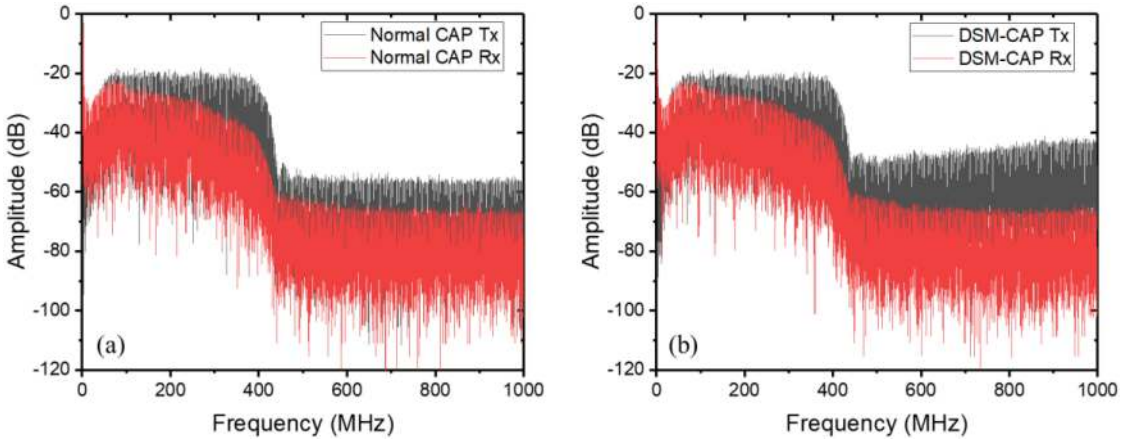

Fig. 4. The spectrum of transmitted signal and received signal: (a) Normal CAP, (b) DSM-CAP.

levels. In this experiment, to make a compromise over signal-to-quantization-noise ratio (SQNR) and oversampling rate, the primary quantization level is set to 4-bit (16 levels), and the OSR is set to 8. Additionally, to avoid the instability of higher order loop filter, we employ 1-order DSM, and the design of loop filter is based on the CLANS methodology [19]. The above process is completed by MATLAB offline. The arbitrary waveform generator (AWG) generates DSM-CAP signals. The spectrum of transmitted signal is shown in Fig. 4. It's clear that the high frequency of DSM-CAP transmitted signal is lifted. After equalization, electrical amplifier (Mini-Circuits ZHL-2-8-S $+$), the signal is coupled with bias current through bias-Tee (Mini-Circuits ZFBT-4R2GW-FT $+$) to drive the LED. The blue chip (457 nm) of a five-color LED (RGBYC LED) [1] is utilized, the output power is 48 mW and the 3 dB bandwidth is 17 MHz.

After 1.2 m underwater transmission, lens and aperture are used to adjust the received optical signal. The water in the tank is tape water. In this paper, the scenario is approximately a deterministic path and the effects of turbulence induced fading could be ignored. At the receiver-side, the PIN (Hamamatsu 10784) implements the optical-to-electrical conversion. The power dissipation of PIN is 50 mW, and the typical 3 dB bandwidth is 300 MHz. To reduce common-mode noise, we utilize differential output. As Fig. 4 shows, for both normal CAP and DSM-CAP, high frequency component displays attenuation. Then the signal is sampled by oscilloscope (OSC). Afterwards, the received signal is sent to offline digital signal processing (DSP) block. The orthogonal shaping filter pair (matched with CAP generation) are used to separate the I/Q components, and after down-sampling by 8 times, an adaptive equalizer based on least mean square (LMS) equalization is employed to compensate ISI distortion, where 2000 training symbols are employed to obtain the

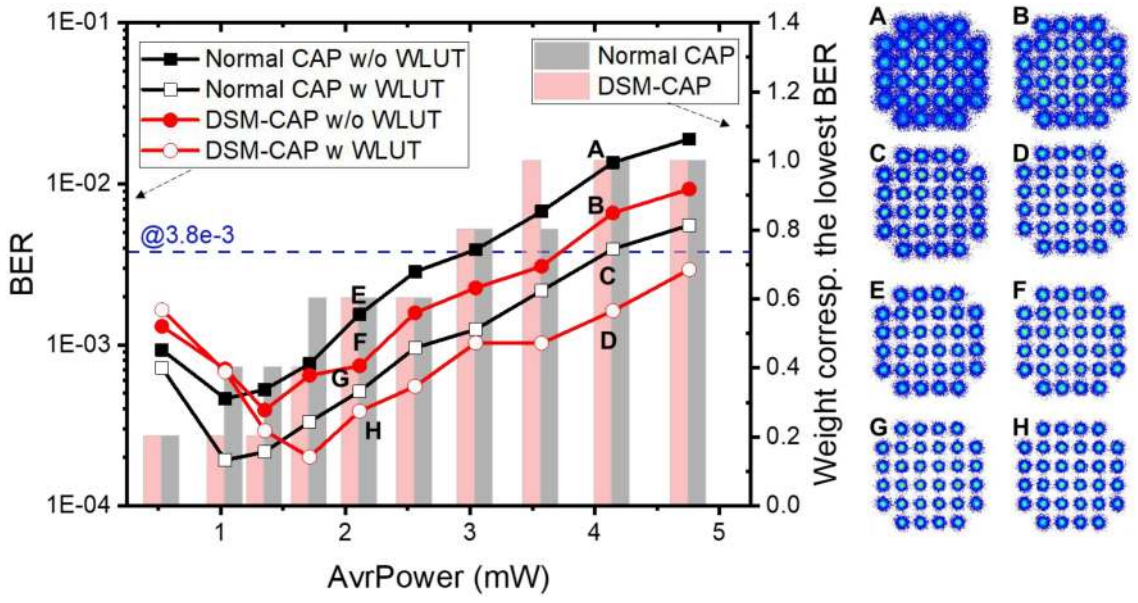

Fig. 5. BER versus average power of transmitted signal.

inverse of the channel response. Then, the table of MP-WLUT is established through 2^{16} training symbols. Afterwards, in the signal distortion phase, LUT could be employed for pre-distortion. For performance measurement, new 2^{16} symbols are pre-distorted and transmitted. The process of MP-WLUT pre-distortion phase is basically the same as MP-WLUT establishing phase. The difference is, at transmitter-side, the QAM mapped signal is pre-distorted, and at receiver-side, the LMS-equalized signal is QAM de-mapped to obtain the original data sequence.

4. Results and Discussion

At first, the performance at different average power of transmitted signal is investigated. As Fig. 5 shows, the bar chart is corresponding to the right axis, indicating the weight corresponding to the lowest BER of WLUT versus average power of transmitted signal, and the curves is corresponding to the left axis, indicating the bit error rate (BER) versus average power of transmitted signal at the weight corresponding to the lowest BER of WLUT. In this experiment, pattern of 3 continuous symbols is investigated. For normal CAP and DSM-CAP, the weight corresponding to the lowest BER decreases as average power of transmitted signal is reduced. Because at low average power, the performance of system is mainly limited by signal-to-noise ratio (SNR). At low average transmitting power, noise is approximately random and has little contribution to prior knowledge of pattern dependent distortion. As the curves show, for both normal CAP and DSM-CAP, signal with WLUT has lower BER except at the average power of 0.5 mW and the weight corresponding to the lowest BER of 0.2, where the performance of DSM-CAP with WLUT is even worse than that without WLUT.

We can also see that at low average power of transmitted signal, the performance of DSM-CAP is no better than normal CAP. Because the DSM-CAP not only suffers noise from UVLC channel as normal CAP, but also partial quantization noise remained in signal band after noise-shaping. However, as the average power increases, the main limitation of system performance is transferred from SNR to nonlinearity, and thus DSM-CAP, with lower PAPR, has better performance at high average power. That is also the reason why all curves display a turning point as the average power increases. Constellations of normal CAP and DSM-CAP with or without WLUT are illustrated on the right part of Fig. 5, where subfigures A, B, C and D are constellations at the average transmitting

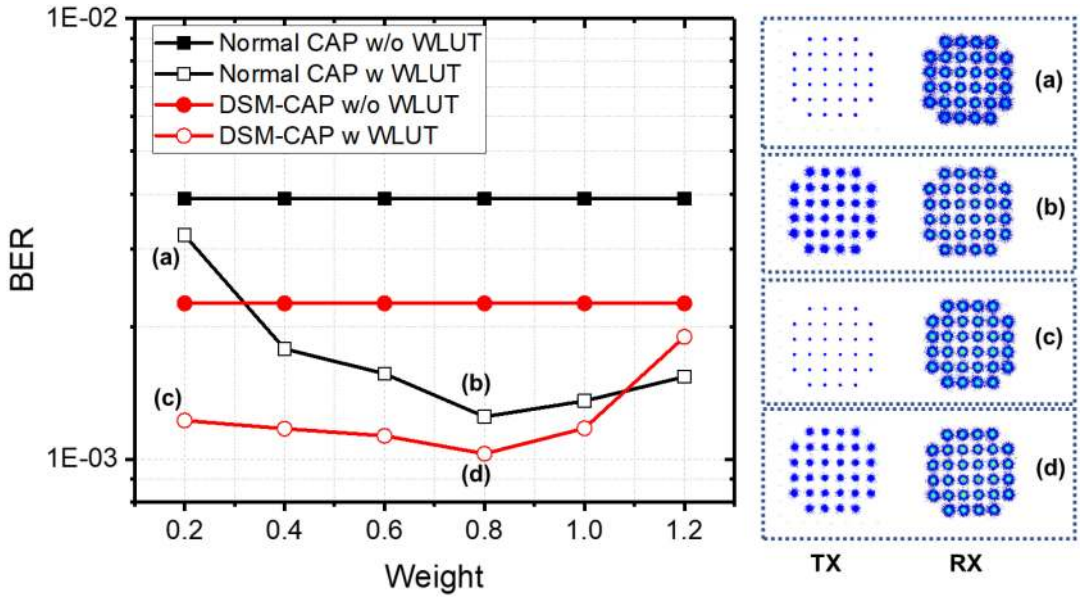

Fig. 6. BER versus the weight of WLUT at the average power of 3.05 Mw.

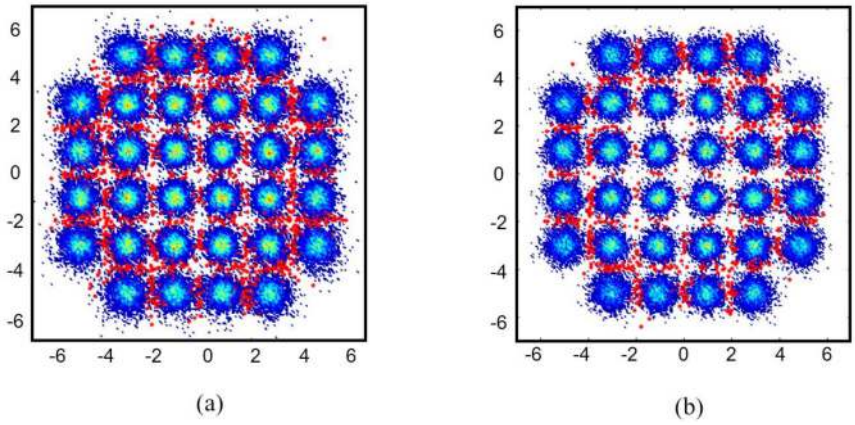

Fig. 7. Constellations of received signal: (a) Normal CAP and (b) DSM-CAP. The red points represent error.

power of 4.1 mW, and subfigures E, F, G and H are at 2.1 mW. Obviously, when the average power is high, the boundary between constellation clusters becomes unclear.

Fig. 6 shows the performance versus weight at the average power of 3.05 mW. Constellations of pre-distorted transmitted signal and received signal are illustrated on the right. When pre-distortion weight is low, the nonlinearity couldn't be fully compensated. As weight increases, BER of normal CAP and DSM-CAP with WLUT decreases. However, the curves with WLUT display a turning point, because random noise exists and ISI couldn't be fully separated owing to limited length of pattern. Enlarging the weight of these components will degrade the performance of WLUT pre-distortion. Therefore, it's necessary to make a compromise. At the current average power, the weight corresponding to the lowest BER is approximately 0.8.

To observe the distortion distribution of Normal CAP and DSM-CAP more clearly, the constellations of received signal are shown in Fig. 7 . Here, the average power of transmitted power is 3.57 mW. The red points represent error. Apparently, subfigure (a) is more scattered than subfigure

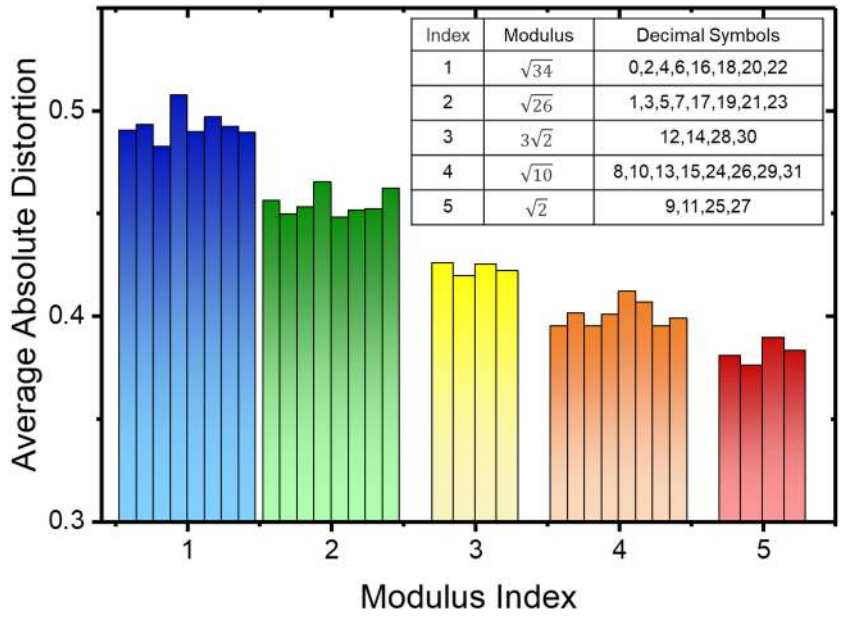

Fig. 8. Average absolute distortion of 32QAM decimal symbols at different modulus. Inset: table of modulus value and corresponding decimal symbols.

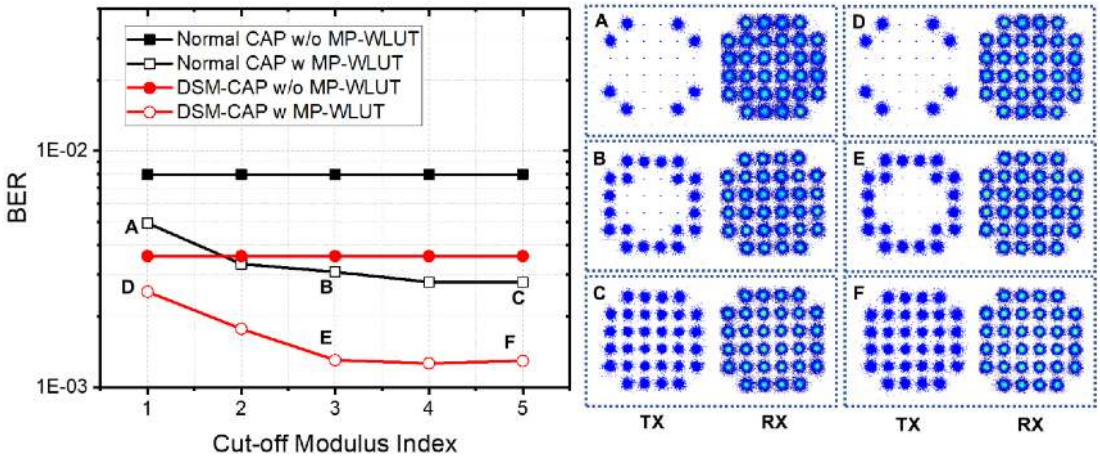

Fig. 9. BER versus cut-off modulus index of MP-WLUT.

(b). For both (a) and (b), error exists more likely at outer modulus. Fig. 8 shows the average absolute distortion (AAD) of symbols after UVLC transmission and the decimal symbols are classified by modulus. The average power is fixed at 3.05 mW. There are 5 moduli for 32-CAP. The index of the outermost modulus is 1, while the index of the innermost modulus is 5. We can see that AAD of symbols at the same modulus fluctuates in a small range, while between different modulus index, there is an obvious gap. As a result, as the modulus index increases, or in other words, as the value of modulus decreases, the AAD diminishes.

Based on the above results, modulus pruned WLUT is proposed. Fig. 9 shows the BER versus cut-off modulus index of pruned WLUT. Constellations of transmitted and received signal at various cut-off modulus index are also illustrated in the figure. As cut-off modulus index increases, more patterns of inner modulus are remained in WLUT, and the BER is reduced. However, we can observe that the decline of BER is retarded when cut-off modulus index transfers from 3 to 5.

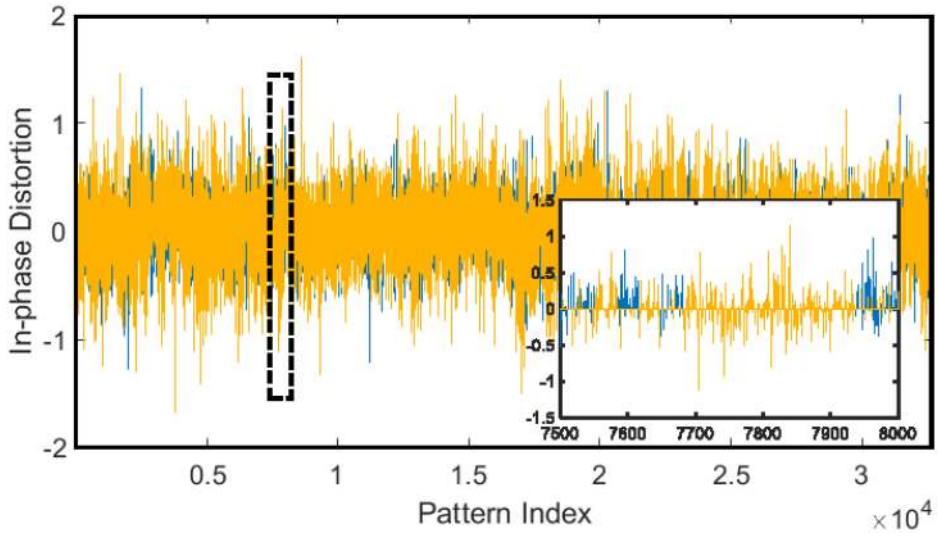

Fig. 10. In-phase distortion recorded in WLUT: full-size (blue) and pruned (yellow).

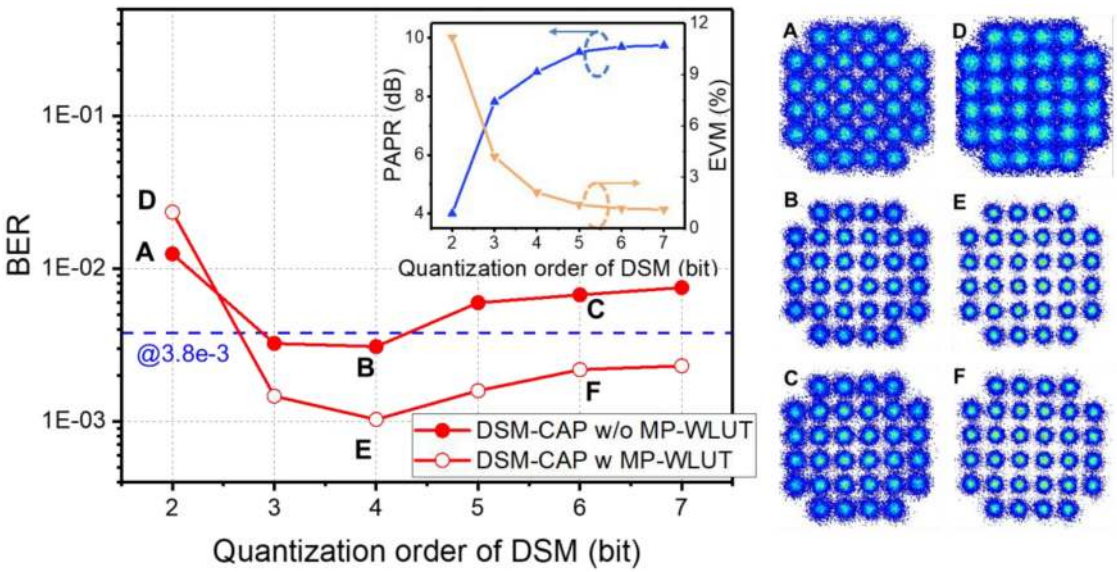

Fig. 11. BER versus quantization order of delta-sigma modulation. Inset: PAPR and EVM versus quantization order of delta-sigma modulation.

Therefore, patterns of which the middle symbol belongs to inner modulus in WLUT only has minor contribution to nonlinearity compensation. In Fig. 10, in-phase distortion recorded in WLUT is illustrated. Blue represents full-size WLUT, and yellow represents MP-WLUT. The cut-off modulus index is 3. Compared with full-size WLUT, the size of MP-WLUT is reduced to 62.5%.

Fig. 11 is BER versus quantization order of delta-sigma modulation. The average power of transmitted signal is fixed at 3.05 mW. The BER curves display a turning point at 4-bit quantization order. The inserted figure is PAPR of transmitted DSM-CAP and error vector magnitude (EVM) versus Quantization order of DSM. PAPR is corrected with resistance to nonlinearity, while EVM is measured between original QAM data and demodulated DSM-CAP through a LPF in simulation, reflecting the level of quantization noise. As the figure indicates, lower quantization order has lower

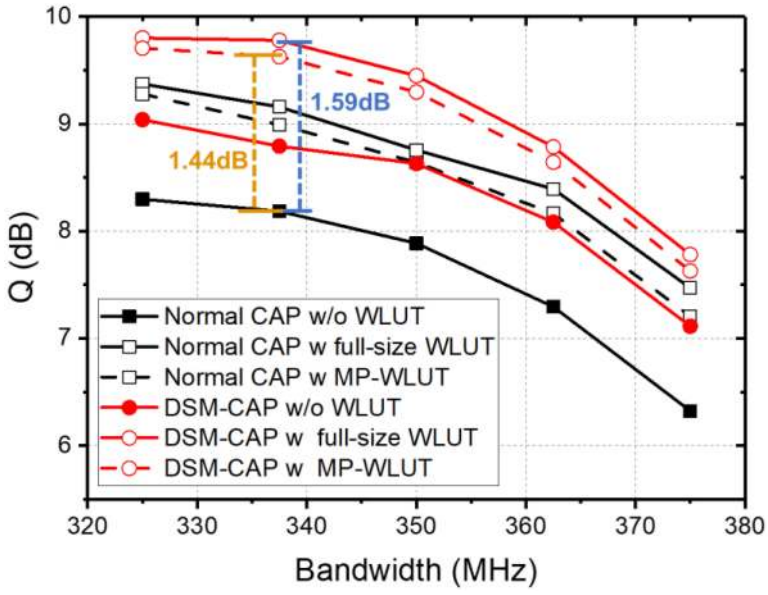

Fig. 12. Q factor versus bandwidth of normal CAP and DSM-CAP.

PAPR but meanwhile more quantization noise is introduced. Constellations displayed on the right also correspond with the conclusion. As a result, 4-bit DSM-CAP has the optimal performance.

Q factor versus bandwidth of normal CAP and DSM-CAP is shown in Fig. 12. Here, the quantization order of DSM is set to 4-bit and the average power of transmitted signal is set to 3.05 mW. The curves of signal without WLUT, with full-size and MP-WLUT for both normal CAP and DSM-CAP are illustrated. The cut-off modulus index of MP-WLUT is 3. For all curves, due to the attenuation response at high frequency in UVLC system, the Q factor decreases as bandwidth becomes higher. Full-size WLUT has the optimal performance. At the bandwidth of 337.5 MHz and the data rate of approximately 1.69 Gbps, employing full-size WLUT pre-distorted DSM-CAP, an improvement of 1.59 dB is realized compared with normal CAP without WLUT. As for modulus pruned WLUT pre-distorted DSM-CAP, the size of WLUT is reduced to 67.5%, while the improvement is 1.44 dB, which is only 0.15 dB below compared with that of full-size WLUT.

5. Conclusion

We proposed and experimentally demonstrated MP-WLUT pre-distorted multi-bit DSM-CAP in UVLC system, where the CAP order is set to 32. Experimental results indicate that DSM-CAP performs well in nonlinearity mitigating. Employing MP-WLUT could further modify the output of delta-sigma modulator through pattern dependent nonlinear pre-distortion. As a result, at the data rate of approximately 1.69 Gbps at the 7% forward error correction (FEC) threshold, compared with normal CAP without WLUT, the Q factor increased by 1.44 dB utilizing MP-WLUT pre-distorted 4-bit DSM-CAP, only 0.15 dB lower than that of full-size WLUT, but the size of WLUT was reduced to 62.5%.

References

[1] Y. Zhou *et al.*, "Common-anode LED on a si substrate for beyond 15 Gbit/s underwater visible light communication," *Photon. Res.*, vol. 7, pp. 1019–1029, 2019.
[2] N. Chi, H. Haas, M. Kavehrad, T. D. C. Little, and X. Huang, "Visible light communications: Demand factors, benefits and opportunities," *IEEE Wireless Commun.*, vol. 22, no. 2, pp. 5–7, Apr. 2015.
[3] N. Chi, Y. Zhou, Y. Wei, and F. Hu, "Visible light communication in 6G: Advances, challenges, and prospects," *IEEE Veh. Technol. Mag.*, vol. 15, no. 4, pp. 93–102, Dec. 2020.

[4] M. Elamassie, F. Miramirkhani, and M. Uysal, "Performance characterization of underwater visible light communication," *IEEE Trans. Commun.*, vol. 67, no. 1, pp. 543–552, Jan. 2019.
[5] N. Chi, Y. Zhao, M. Shi, P. Zou, and X. Lu, "Gaussian kernel-aided deep neural network equalizer utilized in underwater PAM8 visible light communication system," *Opt. Express*, vol. 26, pp. 26700–26712, 2018.
[6] F. Hu *et al.*, "Demonstration of a low-complexity memory-polynomial-aided neural network equalizer for CAP visible-light communication with superluminescent diode," *Opto-Electron. Adv.*, vol. 3, no. 8, 2020, Art. no. 200009.
[7] Y. Wang, L. Tao, X. Huang, J. Shi, and N. Chi, "8-Gb/s RGBY LED-Based WDM VLC system employing high-order CAP modulation and hybrid post equalizer," *IEEE Photon. J.*, vol. 7, no. 6, pp. 1–7, Dec. 2015.
[8] L. Tao, Y. Wang, Y. Gao, A. P. T. Lau, N. Chi, and C. Lu, "Experimental demonstration of 10 Gb/s multi-level carrier-less amplitude and phase modulation for short range optical communication systems," *Opt. Express*, vol. 21, pp. 6459–6465, 2013.
[9] Y. Wang, L. Tao, X. Huang, J. Shi, and N. Chi, "Enhanced performance of a high-speed WDM CAP64 VLC system employing volterra series-based nonlinear equalizer," *IEEE Photon. J.*, vol. 7, no. 3, pp. 1–7, Jun. 2015.
[10] Z. Wang, M. Zhang, S. Chen, and N. Chi, "Carrier-less amplitude and phase modulated visible light communication system based on a constellation-shaping scheme," *Chin. Opt. Lett.*, vol. 15, 2017, Art. no. 030602.
[11] F. Hu, P. Zou, G. Li, W. Yu, and N. Chi, "Enhanced performance of CAP-Modulated visible light communication system utilizing geometric shaping and rotation coding," *IEEE Photon. J.*, vol. 11, no. 5, pp. 1–12, Oct. 2019.
[12] N. Chi, Y. Zhou, S. Liang, F. Wang, J. Li, and Y. Wang, "Enabling technologies for high-speed visible light communication employing CAP modulation," *J. Lightw. Technol.*, vol. 36, pp. 510–518, 2018.
[13] I. Neokosmidis, T. Kamalakis, J. W. Walewski, B. Inan, and T. Sphicopoulos, "Impact of nonlinear LED transfer function on discrete multitone modulation: Analytical approach," *J. Lightw. Technol.*, vol. 27, no. 22, pp. 4970–4978, Nov. 2009.
[14] J. Wang *et al.*, "Delta-sigma modulation for digital mobile fronthaul enabling carrier aggregation of 32 4G-LTE/30 5G-FBMC signals in a single-λ 10-Gb/s IM-DD channel," in *Proc. Opt. Fiber Commun. Conf.*, 2016, Paper W1H.2.
[15] J. Wang *et al.*, "Digital mobile fronthaul based on delta-sigma modulation for 32 LTE carrier aggregation and FBMC signals," *IEEE/OSA J. Opt. Commun. Netw.*, vol. 9, no. 2, pp. A233–A244, Feb. 2017.
[16] H. Qian, J. Chen, S. Yao, Z. Y. Zhang, H. Zhang, and W. Xu, "One-bit sigma-delta modulator for nonlinear visible light communication systems," *IEEE Photon. Technol. Lett.*, vol. 27, no. 4, pp. 419–422, Feb. 2015.
[17] Z. Yu, A. J. Redfern, and G. T. Zhou, "Using delta-sigma modulators in visible light OFDM systems," in *Proc. 23rd Wireless Opt. Commun. Conf.*, 2014, pp. 1–5.
[18] Y. Yoffe *et al.*, "Low-Resolution digital pre-compensation enabled by digital resolution enhancer," *J. Lightw. Technol.*, vol. 37, pp. 1543–1551, 2019.
[19] S. Liang, Z. Jiang, L. Qiao, X. Lu, and N. Chi, "Faster-than-Nyquist precoded CAP modulation visible light communication system based on nonlinear weighted look-up table predistortion," *IEEE Photon. J.*, vol. 10, no. 1, pp. 1–9, Feb. 2018.
[20] N. Chi and F. Hu, "Nonlinear adaptive filters for high-speed LED based underwater visible light communication," *Chin. Opt. Lett.*, vol. 17, 2019, Art. no. 100011.
[21] M. Elamassie and M. Uysal, "Performance characterization of vertical underwater VLC links in the presence of turbulence," in *Proc. 11th Int. Symp. Commun. Syst., Netw. Digit. Signal Process.*, 2018, pp. 1–6.
[22] J. G. Kenney and L. R. Carley, "Design of multibit noise-shaping data converters," *Comput.-Aided Des. Analog Circuits Syst.*, vol. 226, pp. 99–112, 1993.